

---

## Waveform seismic AVAZ responses from orthorhombic models

Sitamai Winnie Ajiduah and Gary Frank Margrave

### SUMMARY

A seismic numerical experiment has been conducted with the goal of analyzing the effect of azimuthal anisotropy in HTI and orthorhombic shale models. A set of parallel vertical fractures embedded in a VTI background in shales leads to orthorhombic anisotropy and seismic AVAZ responses. We compute the elastic anisotropy of shales using elastic parameters and based on TIGER elastic finite difference scheme. We calculate AVAZ responses which consist of PP and mode-converted PSV and PSH reflections. Results indicate the AVAZ from the top interface are distinct from those from the bottom, which reveals the presence of propagation effects. Comparisons between HTI and orthorhombic anisotropy for shales indicate the VTI background may alter AVAZ features of reflections. The expected shear-wave splitting behavior is observed in the acquisition domain of X, Y, and Z component but marred by finite difference artificial noise when rotated back to model domain. This posed a challenge in further analysis of the AVAZ behavior of the S1 and S2 signals.

### INTRODUCTION

Fractures are one of the crucial features in the exploration and exploitation for unconventional shale reservoir. They strongly influence seismic wave propagation, which give rise to fracture-induced anisotropy. They can affect porosity and permeability of reservoirs. Therefore, fracture detection and the estimation of fracture properties are important for reservoir characterization, hydrocarbon production and CO<sub>2</sub> storage. Studies have shown that azimuthal variation in seismic attributes (such as velocity, amplitude, and frequency) of P and S-wave data can be used as an indicator of azimuthal anisotropy (Daley and Hron, 1977; Ruger 1996; Bakulin et. al. 2000; Qian et al., 2007; Mahmoudian, et. al. 2013; Al Dulaijan et. al. 2016). In this study, we investigate a set of parallel vertical fractures embedded in a VTI background. Seismic waves propagating through this type of model will exhibit orthorhombic anisotropy behavior. The objective of this work is to model elastic behavior in 3D azimuthally anisotropic media with the aim of understanding shear wave splitting in real case. i.e. multicomponent surveys over azimuthally anisotropic rocks such as fractured reservoirs. We used TIGER's staggered-grid elastic finite difference scheme to estimate the seismic responses from the interface containing the orthorhombic symmetry. The intention was to be able to simulate S1 and S2 waves emerging from the base of the reservoir. We calculated AVAZ responses of the compressional waves and its mode conversions from the fractured layer and compared the results between HTI symmetry and orthorhombic symmetry. For an excellent comparative review of modern modelling techniques, see Carcione et al. (2002).

### Orthorhombic media

Orthorhombic media are characterized by three mutually orthogonal planes of symmetry. If the axes of a Cartesian reference coordinate system are aligned within the symmetry

planes, i.e., if the coordinate planes coincide with the symmetry planes, the stiffness matrix of the orthorhombic system has nine independent entries and reads (Tsvankin, 2001):

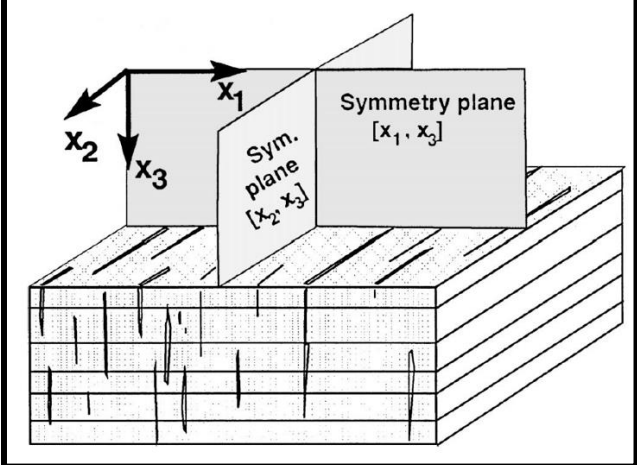
$$C_{IJ}^{\text{Ortho}} = \begin{pmatrix} C_{11} & C_{12} & C_{13} & 0 & 0 & 0 \\ C_{12} & C_{22} & C_{23} & 0 & 0 & 0 \\ C_{13} & C_{23} & C_{33} & 0 & 0 & 0 \\ 0 & 0 & 0 & C_{44} & 0 & 0 \\ 0 & 0 & 0 & 0 & C_{55} & 0 \\ 0 & 0 & 0 & 0 & 0 & C_{66} \end{pmatrix}$$


Figure 1: Symmetry planes in orthorhombic media where anisotropy arises from a system of parallel vertical fractures embedded in a VTI medium, after Tsvankin (2001).

In sedimentary basins, orthorhombic symmetry is commonly caused by parallel vertical fractures embedded within a VTI background medium (Figure 1b). It may also arise due to two or three mutually orthogonal fracture sets, or due to two identical fracture systems crisscrossing with an arbitrary angle (Tsvankin, 1997). Such sets of fractures are common, e.g., for thick sandstone beds and granites. Bakulin et al. (2000b) conclude that orthorhombic symmetry thus might be the most realistic symmetry for many geophysical problems. Despite this conclusion, the application of orthorhombic anisotropy in seismic inversion and processing is obstacle by the large number of nine independent entries of the stiffness matrix. Moreover, if the orientation of the symmetry planes is unknown, as it is usually the case in seismic field experiments the number of unknowns increases to 12, since the angles between the symmetry planes and the coordinate planes of the reference observation system must be determined additionally.

### NUMERICAL EXAMPLES

The SINTEF TIGER 3-D anisotropic elastic finite-difference code was tested on two simple land models consisting of a vertically varying medium in which is embedded an interface of (i.) orthorhombic symmetry in one model and (ii.) HTI symmetry in the second model, with symmetry plane along the x axis. The size of the grid has 201 x 201 x 201

nodes, and the node spacing was  $dx = dy = dz = 20\text{m}$ . The source time function was a Ricker wavelet with a maximum frequency of 40 Hz. The source was in the centre of the xy-plane at depth 20m, and approximately 1080m and 1580m above the embedded fractured layers. Receivers were located approximately 20m below the surface at the same depth as the source. The survey geometry is of orthogonal type and 201 inline receivers and 201 crossline receivers were deployed. A 26-grid point buffer zone was applied on all edges of the grid to minimize edge reflections.

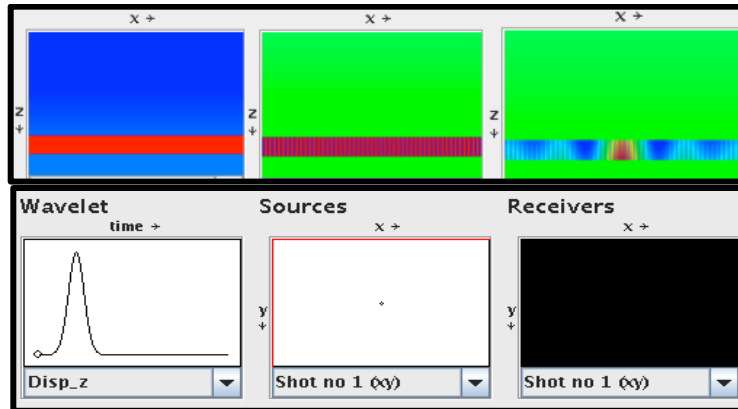


Figure 2: Shows the isotropic, HTI and orthorhombic models used in this work. The later panels show wavelet type and source-receiver geometry. The average velocities of the intermediate layers are designed in a way as to avoid Scholte waves and to reduce edge effect.

Figure 2 shows the design of a reflection model for the study of seismic AVAZ from anisotropic shale reservoirs. In the model, the layer of interest is embedded into two isotropic layers. For comparison, we compute seismic AVAZ responses for the cases of HTI and orthorhombic anisotropy for the shale layer, which corresponds to the cases where a set of vertical fractures are embedded into an isotropic or VTI anisotropic background. The thickness of the shale layer is set as 500m. We then analyze the computed synthetic seismograms of seismic AVAZ in terms of full waveforms consisting of Z-, X- and Y-components and Z, R and T components respectively. Accordingly, Figure 3 illustrates all possible reflections modes, where the symbol S in the isotropic overburden corresponds to SV mode for the R-component and SH mode for the T-component, respectively. The symbol S1 and S2 in the anisotropic shale indicate the split fast and slow shear waves, respectively.

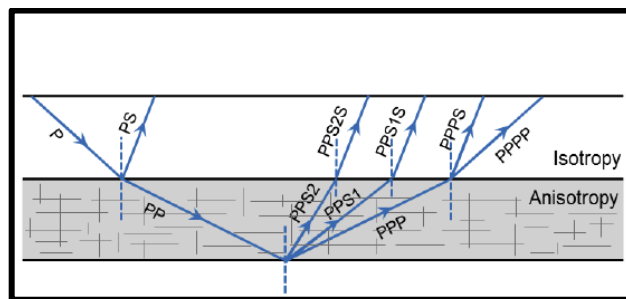


Figure 3: Raypaths for various reflection modes (Wang et.al 2016)

The snapshots and seismic sections are recorded in the vertical x-z-plane and in the vertical y-z plane containing the source. The x-z plane contains the symmetry axis while the y-z plane is the axis containing the isotropy plane. In x-z plane, the y-component is non-zero because the q-SH mode is excited. As expected in a TI medium with horizontal symmetry axis (i.e. HTI or orthorhombic media with horizontal symmetry), the symmetries of the horizontal and vertical components are broken, and all components of the displacement is non-zero in x-z plane (symmetry plane).

## NUMERICAL EXAMPLE

On the seismic sections, we can identify the direct wave, the Scholte wave and six reflected body waves; the (quasi) PP-, PS-, PPPP-, PPPS-, PPS1S- and PPS2S-modes. The travel-time difference between the S1 and S2 modes due to shear wave splitting is of the order 20ms which is less than the period of the waveform. Consequently, identification of S1 and S2 modes as separate events is difficult and the shear wave splitting is observable only as an amplitude effect. As the source receiver offset increases, the quality of the birefringence generated are further degraded by artificial reflections from the boundaries and by the effect of scattering within the anisotropic shale layer.

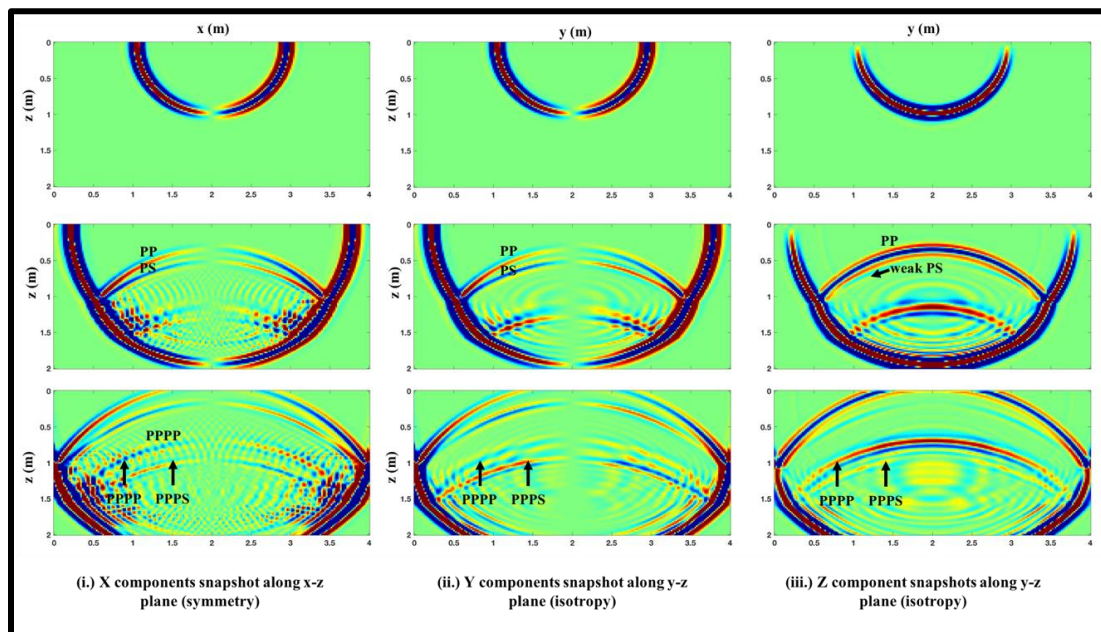


Figure 4. Snapshots of the X-, Y- and Z-component displacement in Orthorhombic model after 0.4, 0.65 and 0.78 seconds.

Figure 5 shows the 3-D finite-difference shot records and comparison of reflection modes and seismic responses of waves propagating in an isotropic, HTI and orthorhombic layers correspondingly. Figure 4(a) shows the shot record generated by isotropic modelling. Both pure reflections (P-P, S-S) and converted wave reflections (P-S, S-P) are easily identified on the in-line (X-component) and vertical (Z-component) receivers. The conversions during transmission are much weaker, and are not annotated. The cross-line (isotropic-layer Y-component) receiver does not record any response, since no SH-wave is

generated in this case. Figure 4(b and c) shows the shot record generated by modeling in the HTI and orthorhombic model. The presence of azimuthal anisotropy in the second layer gives rise to some new features. First, the Y-component responds to reflections arising from both top and bottom of that layer. Second, the wave-modes that are transmitted through this layer ( the later P-S event) are clearly split into two distinct arrivals of S1 and S2 modes and arriving at the receivers as PPS1S and PPS2S modes. This is the evidence of shear-wave splitting.

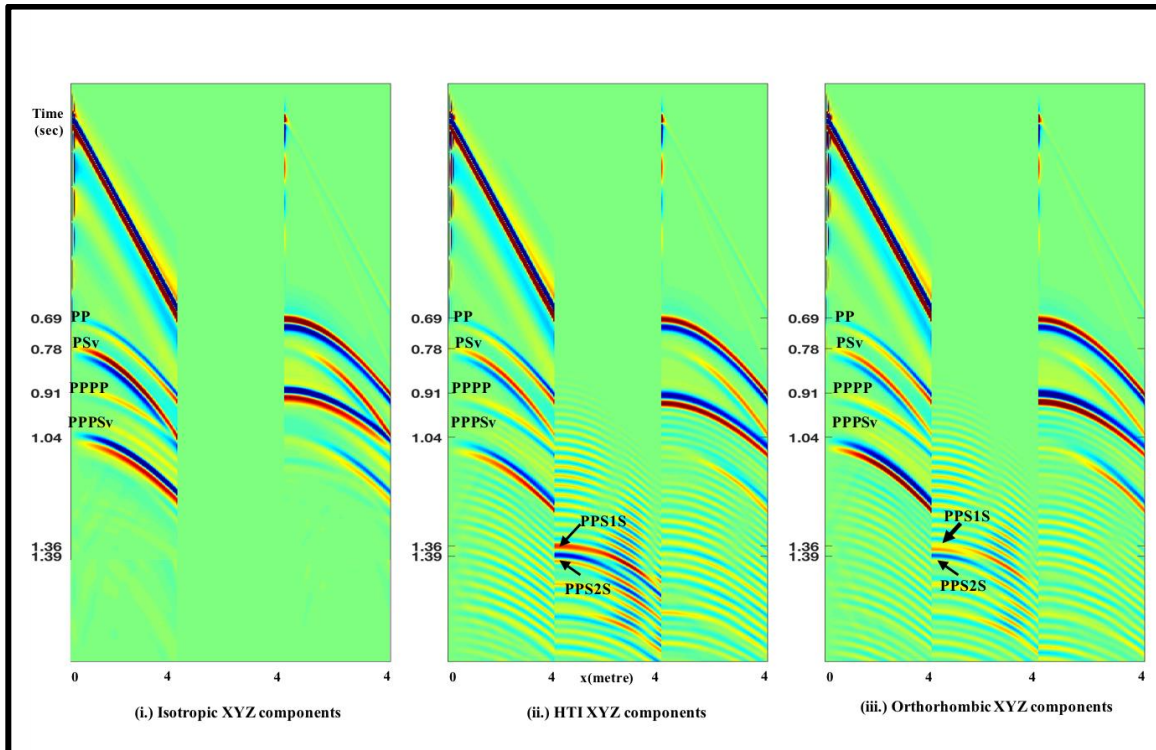


Figure 5: Isotropic vs. HTI modeling in 3-layer medium. X, Y and Z component responses to vertical displacement source over three layered media where second layer is: (i.) isotropic (ii.) HTI with a symmetry axis at  $0^\circ$  to the in-line direction and (iii.) orthorhombic. Events annotated for pure and converted reflections from interfaces A and B. Note the presence of split shear-wave on the PS conversion from interface B in (ii.) and (iii).

Figure 6(i.) and 6(ii.) illustrates the calculated AVAZ responses of P wave reflections for HTI and orthorhombic cases of shales, respectively. The modes PP and PPPP are reflections from the top and bottom of the shales, as indicated in Figure 1. In Figure 6(iii) and 6(iv), we showed the picked amplitudes of the PP and PPPP AVAZ responses corresponding to the P wave reflections from the top and bottom of the HTI and orthorhombic shales. We can see that the fracture strike is parallel to the short axis of P-

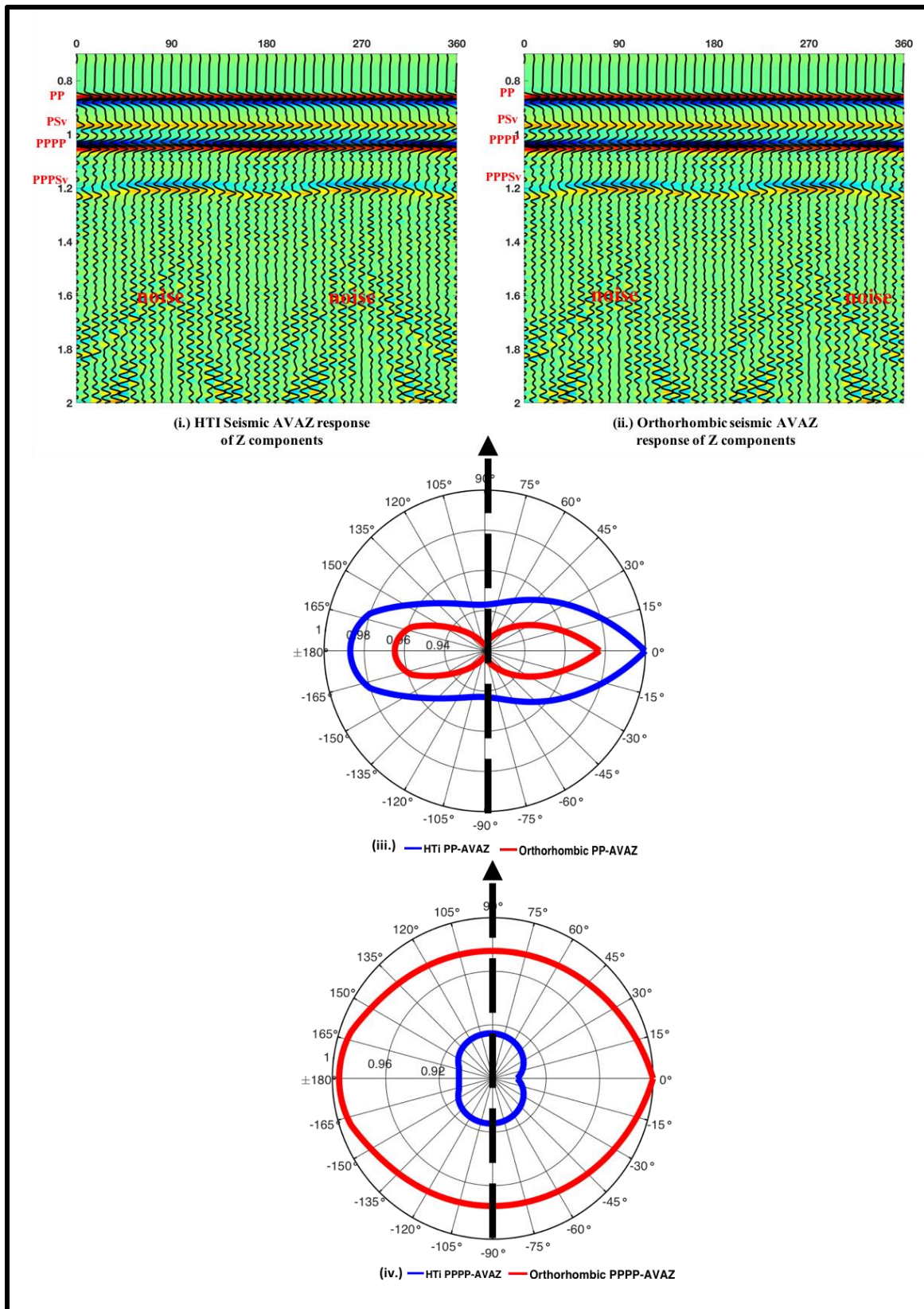


Figure 6: Z-component seismic AVAZ responses from (i.) HTI modeling (ii.) Orthorhombic modeling, and (iii.) AVAZ response from the top interface and (iv.) PPPP

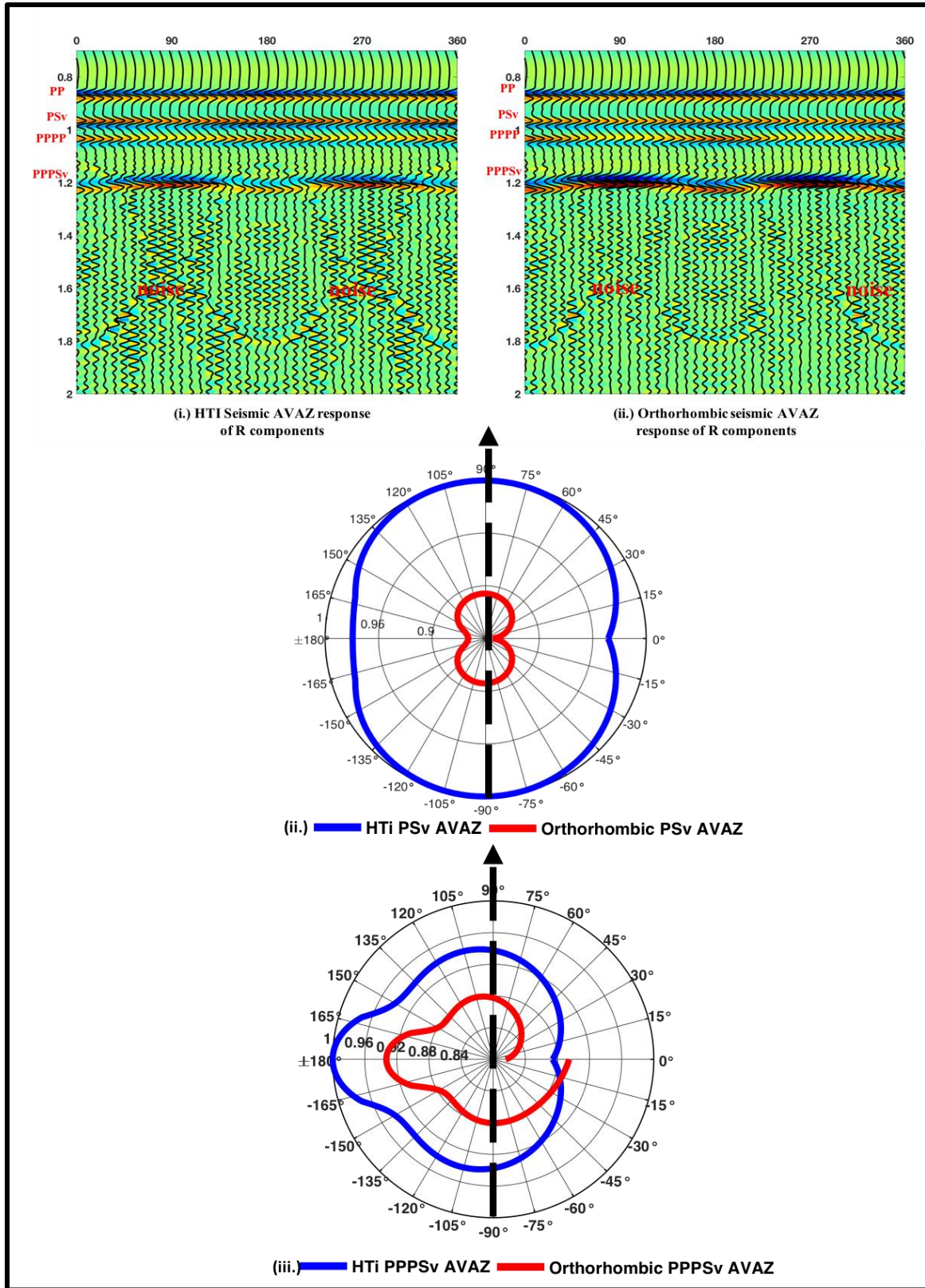


Figure 7: R-component seismic AVAZ responses from (i.) HTI modeling (ii.) Orthorhombic modeling, and (iii.) AVAZ response from the top interface and (iv.) PPPP AVAZ response from the bottom interface of both HTI shale (blue curve) and Orthorhombic shale (red curve).

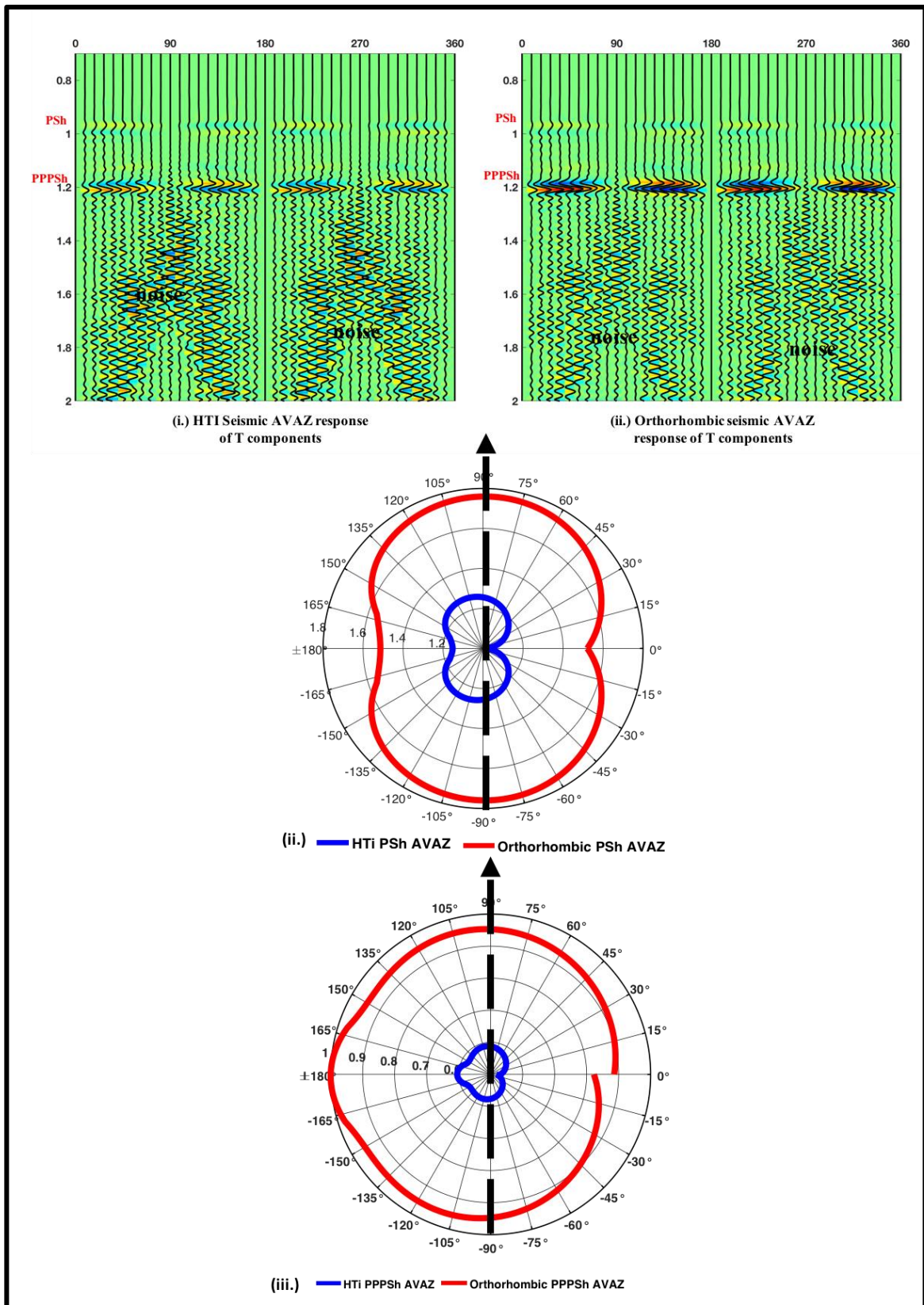


Figure 8: T-component seismic AVAZ responses from (i.) HTI modeling (ii.) Orthorhombic modeling, and (iii.) AVAZ response from the top interface and (iv.) PPPP.

wave AVAZ for top reflections, and by the long axis for bottom reflections. Interestingly, the P-wave AVAZ responses for the HTI and orthorhombic shales are similar for the top reflections but have opposed directions for bottom reflections. This makes it rather challenging to decide fracture orientation from the bottom of an orthorhombic shale layer. In like manner, from Figure 7(i.) to (iv.), we show P-Sv AVAZ responses of R-component, and from Figure 8(i.) to (iv.), we show the P-SH AVAZ responses of T-component. We can observe that the seismic AVAZ of P-SV mode is quite like those of P-SH mode.

## CONCLUSION

We used TIGER 3D numerical modeling work to study seismic AVAZ responses in HTI and orthorhombic shale models and to compare shear wave birefringence from the two shale models. We were able to extract and analyze the PP, PPPP PS and PPS reflections from the top and bottom of the layer, however because of artifacts generated by the TIGER finite difference, the shear wave signals were marred with noise. This noise poses a serious challenge in further analysis of the S1 and S2 signals. In future work, we shall explore other modeling schemes that will preserve the S1 and S2 signals in order to ensure better analysis.

## ACKNOWLEDGMENT

This work was funded by CREWES industrial sponsors and NSERC (Natural Science and Engineering Research Council of Canada) through the grant CRDPJ 461179-13. The authors thank the sponsors of CREWES for continued support.

## REFERENCES

- Al Dulaijan and Margrave, G. F. 2016, VVAZ analysis for seismic anisotropy in the Altamont-Bluebell Field, 86th Annual International Meeting, SEG, Expanded Abstracts.
- Bakulin, A., Grechka, V., and Tsvankin, I., 2000, Estimation of fracture parameters from reflection seismic data. Part I: HTI model due to a single fracture set: *Geophysics*, 65, 1788–1802.
- Carcione, J. M., Herman, G. C. and ten Kroode, A. P. E., 2002, Seismic modelling: *Geophysics* 67, 1304-1325.
- Daley, P.F. and Hron, F., 1977, Reflection and transmission coefficients for transversely isotropic media, *Bulletin of the Seismological Society of America*, 67, 661-675.
- Mahmoudian, F., Margrave, G.F., Wong, J., and Henley, D.C, 2013, Fracture orientation and intensity from AVAZ inversion: A physical modeling study. 83th Annual International Meeting, SEG, Expanded Abstracts.
- Qian, Z., Li, X-Y., Chapman, M., 2007, Azimuthal variations of PP- and PS-wave attributes: a synthetic study: 77th Annual International Meeting, SEG, Expanded Abstracts, 184–187.
- Tsvankin, I. 2001. Seismic signatures and analysis of reflection data in anisotropic media. *Handbook of geophysical exploration: seismic exploration*, vol. 29. Pergamon.
- Wang, P., F. Zhang, S.Q. Chen, et al., 2016, The ODR-dependent attribute analysis of HTI media based on full azimuthal gather: A synthetic study: 86st Annual International Meeting, SEG, Expanded Abstracts, 2314-2318.